

LiMeS-Lab

Citation for published version (APA):

Tanke, V. F. B., Al, R. S., Alonso van der Westen, S., Brons, S., Classen, I. G. J., van Dommelen, J. A. W., van Eck, H. J. N., Geers, M. G. D., Lopes Cardozo, N. J., van der Meiden, H. J., Orrico, C. A., van de Pol, M. J., Riepen, M., Rindt, P., de Rooij, T. P., Scholten, J., Timmer, R. H. M., Vernimmen, J. W. M., Vos, E. G. P., & Morgan, T. W. (2023). LiMeS-Lab: An Integrated Laboratory for the Development of Liquid-Metal Shield Technologies for Fusion Reactors. *Journal of Fusion Energy*, 42(2), Article 44. <https://doi.org/10.1007/s10894-023-00379-3>

Document license:
CC BY

DOI:
[10.1007/s10894-023-00379-3](https://doi.org/10.1007/s10894-023-00379-3)

Document status and date:
Published: 01/12/2023

Document Version:
Publisher's PDF, also known as Version of Record (includes final page, issue and volume numbers)

Please check the document version of this publication:

- A submitted manuscript is the version of the article upon submission and before peer-review. There can be important differences between the submitted version and the official published version of record. People interested in the research are advised to contact the author for the final version of the publication, or visit the DOI to the publisher's website.
- The final author version and the galley proof are versions of the publication after peer review.
- The final published version features the final layout of the paper including the volume, issue and page numbers.

[Link to publication](#)

General rights

Copyright and moral rights for the publications made accessible in the public portal are retained by the authors and/or other copyright owners and it is a condition of accessing publications that users recognise and abide by the legal requirements associated with these rights.

- Users may download and print one copy of any publication from the public portal for the purpose of private study or research.
- You may not further distribute the material or use it for any profit-making activity or commercial gain
- You may freely distribute the URL identifying the publication in the public portal.

If the publication is distributed under the terms of Article 25fa of the Dutch Copyright Act, indicated by the "Taverne" license above, please follow below link for the End User Agreement:

www.tue.nl/taverne

Take down policy

If you believe that this document breaches copyright please contact us at:

openaccess@tue.nl

providing details and we will investigate your claim.



LiMeS-Lab: An Integrated Laboratory for the Development of Liquid–Metal Shield Technologies for Fusion Reactors

V. F. B. Tanke¹ · R. S. Al¹ · S. Alonso van der Westen¹ · S. Brons¹ · I. G. J. Classen¹ · J. A. W. van Dommelen² · H. J. N. van Eck¹ · M. G. D. Geers² · N. J. Lopes Cardozo³ · H. J. van der Meiden¹ · C. A. Orrico³ · M. J. van de Pol¹ · M. Riepen⁴ · P. Rindt³ · T. P. de Rooij³ · J. Scholten¹ · R. H. M. Timmer¹ · J. W. M. Vernimmen¹ · E. G. P. Vos¹ · T. W. Morgan^{1,3}

Accepted: 2 August 2023
© The Author(s) 2023

Abstract

The liquid metal shield laboratory (LiMeS-Lab) will provide the infrastructure to develop, test, and compare liquid metal divertor designs for future fusion reactors. The main research topics of LiMeS-lab will be liquid metal interactions with the substrate material of the divertor, the continuous circulation and capillary refilling of the liquid metal during intense plasma heat loading and the retention of plasma particles in the liquid metal. To facilitate the research, four new devices are in development at the Dutch Institute for Fundamental Energy Research and the Eindhoven University of Technology: LiMeS-AM: a custom metal 3D printer based on powder bed fusion; LiMeS-Wetting, a plasma device to study the wetting of liquid metals on various substrates with different surface treatments; LiMeS-PSI, a linear plasma generator specifically adapted to operate continuous liquid metal loops. Special diagnostic protection will also be implemented to perform measurements in long duration shots without being affected by the liquid metal vapor; LiMeS-TDS, a thermal desorption spectroscopy system to characterize deuterium retention in a metal vapor environment. Each of these devices has specific challenges due to the presence and deposition of metal vapors that need to be addressed in order to function. In this paper, an overview of LiMeS-Lab will be given and the conceptual designs of the last three devices will be presented.

Keywords Fusion technology · Plasma-facing components · Liquid metals · Lithium · Tin

Introduction

Tungsten is considered the baseline divertor plasma facing material (PFM) for many conceptual designs of DEMO-scale fusion reactors [1–3]. While for a quiescent and steady plasma and heat load tungsten appears to fulfil the

necessary requirements, large edge localized modes (ELMs) and disruptions, combined with the very high neutron loads and operational timelines in such devices, may make long-term operation with such a divertor untenable. Liquid metals (LMs) have been widely studied as alternative PFMs that avoid many of the problems associated with the use of tungsten or other solid PFMs [4]. Liquid tin (Sn) or lithium (Li) are generally considered the leading candidates for this approach. Several recent reviews detail the progress and remaining issues in liquid metal research for fusion [5–7]. One important open question is the development of technological solutions for the application of LMs in fusion reactors. Of main concern is that an open fluid surface is strongly vulnerable to destabilization by magnetohydrodynamic forces which can lead to plasma disruption [8]. Currently several different concepts have been developed and tested to prove the possibility of liquid metals as PFCs. Two main solutions

✉ T. W. Morgan
T.W.Morgan@diffier.nl

¹ Dutch Institute for Fundamental Energy Research, De Zaal
20, 5612 AJ Eindhoven, The Netherlands

² Department of Mechanical Engineering, Eindhoven
University of Technology, Groene Loper 3,
5612 AE Eindhoven, The Netherlands

³ Science and Technology of Nuclear Fusion, Eindhoven
University of Technology, Groene Loper 3,
5612 AE Eindhoven, The Netherlands

⁴ ASML, De Run 6501, 5504 DR Veldhoven, The Netherlands

are a thermoelectric magnetohydrodynamics driven fast flowing fluid between metal trenches on the PFC [9] and a capillary porous structure (CPS) which holds the metal via capillary pressure [10]. Some possible reactor implementations for these solutions consist of an externally cooled LM filled CPS plate resupplied via a recirculating loop [4]; A box or baffled divertor structure with a high density lithium vapour cloud to cool the plasma while limiting metal vapor flows to the core plasma [11]; and the flowing lithium liquid limiter tested at the EAST tokamak [12].

While the aforementioned concepts have shown promise, compared to current day solid armor walls, LM-based technology is less ready and is technologically more complex. Current levels of knowledge would not be sufficient to confidently introduce this technology to a multi-billion Euro large scale fusion reactor. Therefore a stepping stone approach to develop this technology to a higher level of readiness via further scientific and technological investigation and improvement is proposed. To date, although many tokamak experiments using liquid metals have successfully taken place [13–16], experiments with liquid metal divertors in medium and large-scale tokamak experimental facilities are lacking. However, the results from these devices would be the best way to confidently extrapolate to DEMO generation reactors. This lack is mainly due to the absence of well-developed and reliable liquid-metal based divertor plasma-facing components (PFCs). Typically, solid PFC designs are tested in high-heat flux and plasma loading facilities [17–19]. However, LM PFCs specifically require high temperature coolants and liquid metal supply loops which do not exist within current facilities of this type, and the liquid metal can contaminate the vacuum systems and diagnostic ports of multi-purpose facilities. Therefore, this project will develop a dedicated liquid metal laboratory which can provide the link between small scale prototype development and larger-scale deployment. Although this project will predominantly focus on the CPS concept for LM-PFCs, the laboratory will also be instrumental for studying other LM PFC concepts such as the previously mentioned box divertor and flowing designs.

Within this liquid metal laboratory, the current liquid metal CPS divertor concepts can further mature to technology suitable for future reactors, by addressing the following challenges:

- Reliably producing tungsten capillary porous structures (CPS) with optimal pore sizes and high strength by means of additive manufacturing.
- Wetting and filling of manufactured CPS targets with the liquid metal in order to take advantage of the capillary refilling during operation.

- Liquid surface stability and heat load handling capability of a circulating liquid metal in a CPS target design under plasma exposure.
- Retention of hydrogen isotopes by the liquid metal and the prevention of impurity formation in the liquid metal that can result in clogging.

The Liquid Metal Shield Laboratory (LiMeS-Lab) aims to provide the infrastructure to address each challenge for different liquid metal divertor concepts, using the liquid metals tin and lithium. To achieve this LiMeS-Lab will consist of 4 devices: A selective laser sintering 3D metal printer (LiMeS-AM), a plasma assisted wetting device (LiMeS-Wetting), a liquid metal loop linear plasma generator (LiMeS-PSI), and a liquid metal compatible thermal desorption spectroscopy system (LiMeS-TDS). At the Dutch Institute for Fundamental Energy Research (DIFFER) and Eindhoven University of Technology (TU/e), these devices are in development. Their functions, driving design concepts and major components will be discussed.

LiMeS-AM

Recent work at DIFFER and TU/e has resulted in promising designs where the CPS structure is produced by additive manufacturing (AM) [20]. This has the advantage that the structure can be tailored to optimize surface tension effects, capillary action liquid metal flow and stress minimization, as well as enabling good thermal contact by direct printing to the cooling pipe. However, additively manufactured tungsten is vulnerable to microcrack formation which strongly reduces its yield strength and toughness [20, 21]. These properties should be maximized for use as a PFC despite the strongly lowered stresses in a sponge-like print compared to a fully solid block. To mitigate this, substrate pre-heating [21, 22] and minimization of oxygen content [22, 23] are proposed as effective levers. Additionally, to print the small feature size required for good capillary restraint [24] a high laser power density is required.

The LiMeS-AM system consists of a Laser Powder Bed Fusion device. By combining a 1000 W single mode fibre laser with a micro-optics system that produces a feature size down to 50 μm , a high power density can be achieved, permitting a large range of process conditions such as spot size, writing speed and layer thickness to be used. A heated build platform up to 800 $^{\circ}\text{C}$ enables printing at temperatures above the Brittle to Ductile Transition Temperature and should reduce stresses in the component and increase the relative mass density [21]. A controlled atmosphere and use of an inerted sieving station enables an oxygen content

below 100 ppm which should help to also reduce cracking [25].

An additive manufacturing device conforming to these specifications is currently under procurement.

LiMeS-Wetting

In order to fill a CPS with a LM, the interaction between the CPS surface and the LM must be stronger than the interaction within the LM. These interactions are determined by the physical properties of the LM and the surface properties of the CPS. The process is characterized by the contact angle and wetting is stated to occur when this angle is less than 90° [26]. The high surface tension of the LM and the inherent roughness of a CPS surface render the wetting a complicated task. However, the naturally present layer of tungsten oxide is not wetted by the liquid metal and prevents the filling of the CPS [26]. Even at room temperature, a 1 nm thick layer of oxide is formed within one hour [27]. Therefore, in order for the liquid metal to wet the CPS, the oxide must first be removed. This can be done by heating the surface sufficiently for the LM to react with the oxide layer and expose the pure metal underneath, or by heating to such a degree that the oxides on the surface are reduced and only pure metal remains [26]. Lithium reacts with the tungsten oxide, requiring only moderately elevated temperatures of around 400°C to achieve wetting. Tin does not show this behaviour. However, vacuum furnace treatment above 900°C has been found to lead to wetting. These high temperatures are not compatible with the other construction materials of a PFC, such as copper for cooling pipes and stainless steel for supporting structures. This would inhibit the development of wetted PFCs for testing.

However, wetting of the CPS surface by tin can be enhanced by introducing hydrogen during the wetting procedure. Recent work using a hydrogen atom source has shown that by exposing a tungsten CPS to a hydrogen radical cloud, wetting of liquid tin on tungsten samples will occur at lower temperatures, 750°C , while filling of the CPS after wetting can be done at 500°C . A pre-treatment of the surface with hydrochloric acid in combination with the above atom source decreased the wetting and filling temperatures to about 420°C . Photos taken during the these experiments can be seen in Fig. 1.

LiMeS-Lab will incorporate a dedicated wetting device (LiMeS-Wetting) that will be capable of wetting a large-scale PFC-mock-up (up to $15 \times 6 \times 3$ cm) with liquid tin, and enable dedicated studies on the wetting behaviour of tin on a variety of surface materials exposed to different surface treatments and wetting environments. A plasma

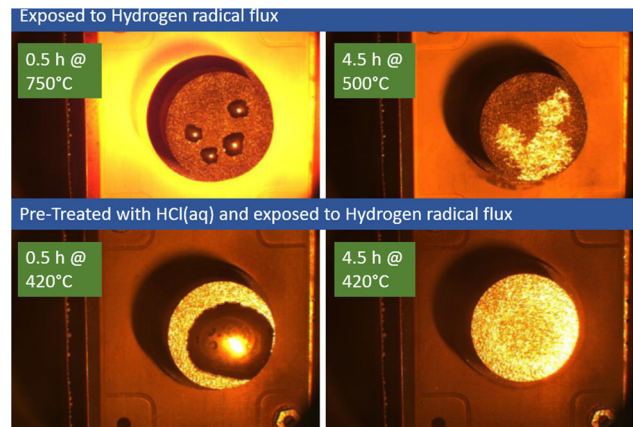


Fig. 1 Photos taken during the filling of tungsten CPS targets with tin while exposed to a hydrogen radical flux (top) and while pre-treated with HCl(aq) and exposed to hydrogen radical flux (bottom). Time expired and temperature are indicated in the photo

source, rather than atom source, will be used to study the effect of hydrogen ions on the wetting of tin on these plasma cleaned surfaces. The device's working principle is to place mock-up PFCs on a heated rail system, exposure the surface to plasma and subsequently inject tin droplets onto the surface to attempt wetting of the CPS. To achieve this, the device will consist of the following components:

- Vacuum chamber and vacuum pumps: To prevent re-oxidation of the CPS surface after treatment as well as create the environment necessary for the plasma source.
- Target manipulator: To move the target between the plasma source and the injector, a transfer arm will be included. This arm drives a carriage on rails on which a target will be placed. This system will also include thermocouple connections to be able to measure the temperature of the target in operation. The target will be placed on the carriage via a quick access door mounted on the vacuum vessel.
- Plasma source: A cascaded arc plasma source [28, 29] similar to that used by Vijvers et al. [30]. The plasma source has been previously characterized under similar experimental conditions as planned here to provide a high flux of radicals ($\sim 10^{22} \text{ m}^{-2}\text{s}^{-1}$) and ions ($\sim 10^{19} \text{ m}^{-2}\text{s}^{-1}$) [31]. The ion flux of the plasma source will be characterized via a Langmuir probe while the radical flux of the plasma source will be measured by a dual-thermopile radical probe [32].
- Liquid metal injector: The injector is used to inject pure metal droplets onto a cleaned surface from a heated reservoir. Due to the small injection orifice, impurities, such as oxides from the tin pellets that are used to fill the reservoir, do not flow out and remain behind in the injector reservoir [33].

- **High temperature heater:** In order to reach the elevated temperatures needed for wetting mentioned previously, a heating system is incorporated into the vessel. To guarantee wetting of targets in all cases, the heater must achieve a target temperature of 1000 °C, so that tungsten oxide reduction via sublimation remains possible. To be able to heat the target under the plasma source for cleaning as well as under the injector for wetting, the heater will consist of several independent modules spanning the vessel. To prevent the vessel from heating up due to the high temperature heater, active cooling of the vessel walls is included.

A conceptual design of the LiMeS-Wetting device, including all previously mentioned components, is shown in Fig. 2. The liquid metal injector and the large high temperature heater will be developed in house.

LiMeS-PSI

At the center of LiMeS-lab is a new linear plasma device dedicated to the plasma exposure of liquid metal targets. The device is intended to investigate several physics aspects of plasma-liquid metal interaction, ranging from vapor-plasma interactions to the dynamics of droplet formation and ejection, and to the retention of plasma species in the liquid and its substrate. Second, the device is intended to aid in technology development of realistic liquid metal divertors for future fusion reactors. This is done by evaluating the performance of liquid metal component mock-ups under a range of exposure conditions, so

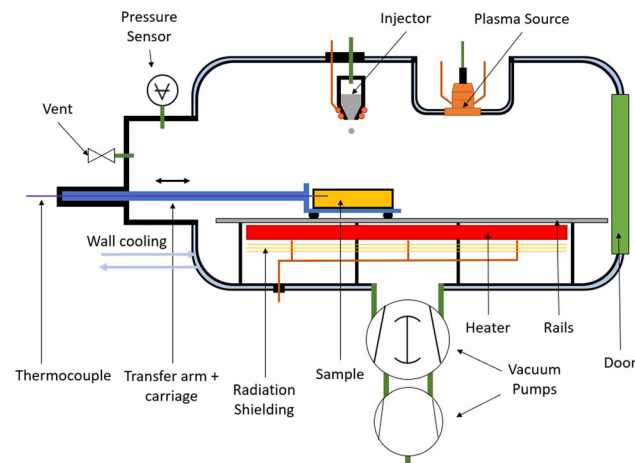


Fig. 2 Concept design of LiMeS-Wetting, with all major components indicated. The device consists of three main stages where a process step can be performed: Plasma cleaning or radical cleaning followed by wetting via the injector. The heater spans the length of the vessel to allow for high temperature operation during any of the process steps. With a design temperature of 1000 °C, water cooling of the vessels walls is included

that they can be improved or qualified for real use. It therefore needs to fulfil the following scientific requirements:

1. A sufficiently high steady-state heat flux plasma to simulate the expected loading conditions in the DEMO divertor.
2. Conditions where vapour-shielding effects strongly influence the plasma. This typically requires relatively small mean-free paths [34] such that a relatively high density plasma is required.
3. Capability of testing the concept of resupply and flow of liquid metal into, through and out of the sample for a representative amount of time for the concept being tested.
4. Compatibility with mock-ups of DEMO representative designs.

LiMeS-PSI will utilize a cascaded arc plasma source, operated in a maximum background pressure of 2 Pa, and a 1.5T superconducting magnet to create a continuous plasma beam with an electron temperature and density of up to 5 eV and 10^{20} m^{-3} . This results in a particle flux of $> 10^{24} \text{ m}^{-2}\text{s}^{-1}$ and a maximum heat flux over 20 MWm^{-2} . DIFFER also operates the Magnum-PSI [35] and UPP linear devices. However compared to these, LiMeS-PSI will integrate the following unique aspects to facilitate the research into liquid lithium and tin plasma facing components:

- A high temperature oil heating/cooling system. By using a lithium compatible oil as a cooling fluid, targets placed in LiMeS-PSI can be heated to 250 °C to melt the lithium ($T_{\text{melt}} = 180.5 \text{ °C}$) or tin ($T_{\text{melt}} = 232 \text{ °C}$) inside the samples and present a liquid surface before plasma exposure. During plasma exposure, the oil can be used to remove the plasma power deposited on the target. Secondly, oil does not react violently with lithium, which is the case for water, providing a safer experimental test device.
- A target holder integrated circulating liquid metal supply system. The system will allow for continuous refill of the liquid metal filled CPS target with a reservoir for 200 g of lithium or 2 kg of tin. To accommodate the liquid metal loops in LiMeS-PSI, mounting points, power lines and diagnostics feed-throughs will be included on the interface between target holder and LiMeS-PSI. The flexible design of this interface allows for the testing of different liquid metal divertor concepts.
- Liquid metal vapor protected diagnostics. The current experience of the use of liquid metal targets at reactor relevant conditions is significant metal vapor deposition on the vacuum vessel windows, especially for lithium

due to low vapor pressure. Simple estimates show that around a 10 nm layer of Li or a 5 nm layer of Sn leads to around a 50% loss in transmission in the visible spectrum, disabling all the diagnostics relying on optical access. In LiMeS-PSI, the diagnostics will be integrated in dedicated port systems utilizing mirrors, aperatures and shutters to prevent deposition of metal vapor on any vacuum vessel windows. With these measures taken, the diagnostics of LiMeS-PSI should be operational until the liquid metal reservoir is completely drained.

- Exchange of targets under protected atmosphere. As lithium is highly reactive with air, samples will be transferred in inert gas suitcases via a transfer chamber into LiMeS-PSI. Using glovebox style gloves, samples can be mounted on the target manipulator within the protected atmosphere. After plasma exposure, the gloves and the suitcase allows for clean transport of targets to a post-mortem analysis device, e.g. to study the retention of hydrogen and deuterium.
- As liquid metal vapor will be deposited over the entirety of the machine due to evaporation (lithium) and droplet ejection (tin), including the first mirrors used for the diagnostics, regular cleaning of LiMeS-PSI will be required. To facilitate the cleaning, LiMeS-PSI will be designed to be easily opened with all critical components in easily reached locations.

The current concept of LiMeS-PSI that integrates all aforementioned aspects is shown in Fig. 3, with the different chambers indicated and the most important

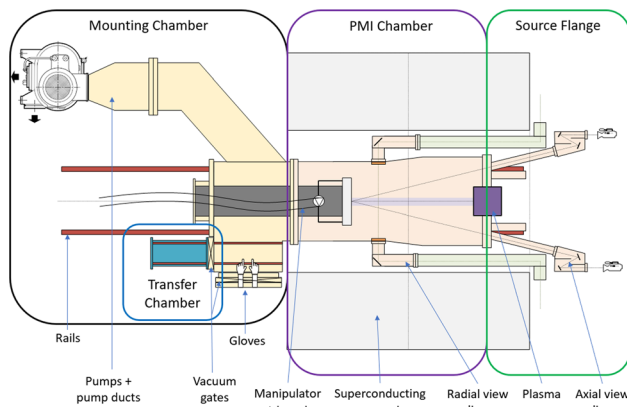


Fig. 3 Concept design of the LiMeS-PSI device. The device consists of a mounting chamber that facilitates mounting of targets in an argon atmosphere with the help of a transfer chamber and gloves. A manipulator will move the target to the plasma exposure position in the PMI chamber, which is surrounded by the superconducting magnet. The PMI chamber is actively cooled and will have several radial port systems that provides protected view lines parallel to the target surface. At the back of the PMI chamber, a large vacuum flange is mounted that will incorporate the plasma source as well as axial port systems that provide a protected view of the target surface

components highlighted. The manipulator indicated in Fig. 3 will house the target holder and electrical feed-throughs for the loop systems and thermocouples for use in LiMeS-PSI, as well as provide the capability of axial scans by the diagnostics on the radial view lines. The axial and radial port systems will provide sufficient view lines for the simultaneous operation of the following diagnostics:

- Thomson scattering (Radial): To measure radial profiles of electron density and temperature.
- Optical emission spectroscopy (Radial & Axial): To capture emission from the plasma.
- Fast visible light camera (Radial): To visualize droplet ejection from the liquid metal surface.
- Absorption shadowgraphy (Radial): To investigate the metal vapor cloud.
- Infrared Camera (Axial): To determine the target surface temperature distribution.
- Pyrometer (Axial): To measure the target surface temperature at a single spot.
- Video Camera (Axial): To provide a view inside the system during operation.

The axial port systems also provide a means for using a high power laser to simulate the transient heat flux of ELMs [19, 36]. Additionally, the mounting chamber used for the exchange of targets will also incorporate vessel ports and infrastructure to accommodate an in-situ laser induced breakdown spectroscopy diagnostic for use after target exposure and before venting the vessel with argon.

Currently, the diagnostic port systems are under development to provide a design that can effectively protect the vacuum vessel windows from the metal vapor depositions.

LiMeS-TDS

In order to characterize hydrogen and deuterium retention in the liquid metal samples exposed in LiMeS-PSI, thermal desorption spectroscopy (TDS) will be used as a post mortem diagnostic. One of the problems encountered in using TDS for liquid lithium samples is the high partial gas pressure due to evaporation of lithium at moderate to high temperature, and the evaporation of tin at very high temperatures. These high pressures are incompatible with the operating range of a typical quadropole mass spectrometer (QMS), the diagnostic used to measure the partial gas pressures. Secondly, there is a possibility of interaction between deposited lithium which was previously evaporated and the hydrogen or deuterium desorbed from the sample. This could result in a continuous hydrogen signal during the TDS procedure, which has been observed during previous experiments with the current TDS device located

at DIFFER. This could be explained by the presence of surfaces in the device with a temperature between the melting point of the liquid metal and the temperature of the sample, e.g. the heat shields around the heater.

This situation can be avoided by using small amounts of lithium, a limited temperature range with a small heater and high heat capacity vacuum vessels, as done in previously reported work [37, 38]. However, LiMeS-TDS must accommodate samples filled with up to 5 g of lithium and 70 g of tin as well as reach a temperature of up to 1000 °C, ruling out the mentioned mitigation strategies. Finally, previous experience has shown that liquid metal vapors, especially tin, will over time corrode and degrade electrical connections and delicate components. Therefore, to prevent all aforementioned problems, LiMeS-TDS will capture all liquid metal vapor on a dedicated actively cooled cold trap.

In order to achieve a cold trap that captures all liquid metal vapors, without creating intermediate temperature surfaces, and shield all delicate components, a double vacuum vessel design is planned. The general idea behind the concept is shown in Fig. 4. The cold trap that is created consists of the following two vacuum chambers:

- The evaporation chamber: A water cooled vacuum chamber to keep the inside vessel temperature below 50 °C, while a sample and heater system located in the center are radiating and evaporating metal vapor at 1000 °C. This chamber will only have one bottom port to prevent depositing liquid metal on any other surface than the directly cooled vessel wall.
- The measurement chamber: located below the evaporation chamber. This chamber will be used to mount all components needed to make the TDS device work. A

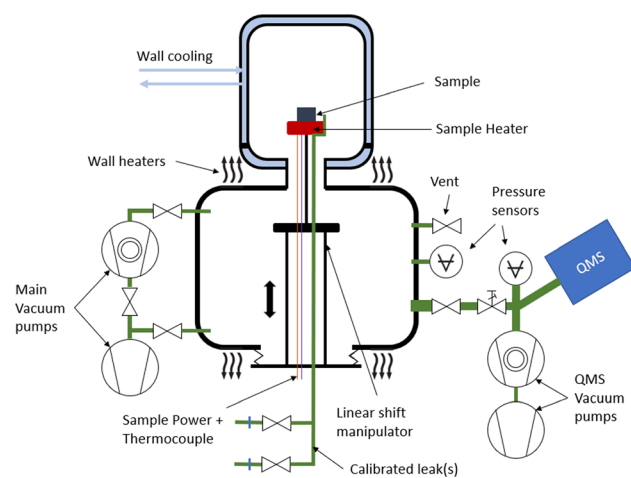


Fig. 4 Concept design of the LiMeS-TDS device, illustrating the double vessel design for the separation of the metal vapor and the hydrogen/deuterium. All major components are indicated. The linear shift manipulator facilitates the movement between the two vessels

sample heater is mounted on a linear shift manipulator. Via the manipulator, the heater and sample can be moved between the measurement chamber and the evaporation chamber. The manipulator also houses and protects the electrical connections and calibration gas lines needed at the sample location.

The heater system, located in the evaporation chamber during operation, will have a diameter that is slightly smaller than the inner diameter of the port connecting the two chambers. As liquid metal will only evaporate from the top surface of the sample, all evaporated metal vapor will first encounter the cooled vessel wall, before being able to escape through the bottom port. Since the sticking coefficient of the metal vapor is close to unity for a cold surface [39], none of the metal vapor should be able to leave the evaporation chamber. In comparison, the sticking coefficient for molecular deuterium is assumed to be zero, as co-deposition with the metal vapor is immeasurably small [40] and the chemical reaction between lithium and molecular hydrogen only becomes relevant at higher temperatures [41]. In this way, the heater acts as a mask for the connection to the other chamber, preventing metal vapor from entering the measurement chamber, while allowing the deuterium to freely flow to the measurement chamber due to the difference in sticking coefficient to the vessel walls. The capturing of the metal vapor and freely flowing hydrogen in this geometry is confirmed using the Direct Simulation Monte Carlo (DSMC) code SPARTA [42]. SPARTA has previously been used to predict lithium transport in vacuum environments [43]. The results of the simulation for lithium vapor and hydrogen gas are shown in Fig. 5. Via the double vessel design, all liquid metal can be captured before it can condense on any incompatible components without significantly influencing the measurement sensitivity of the TDS system.

As lithium can react with hydrogen atoms in a 1:1 ratio, a plasma exposed sample can contain a significant amount of hydrogen. Therefore, depending on the pump used in the device as well as the volume of the vessel, the hydrogen pressure, created by the desorption from the sample, alone can exceed the operation range of the QMS, which is 0.01 Pa. To reduce the pressure to operational range, a differentially pumped chamber will be connected to the measurement chamber where the QMS will be located. By restricting the flow between the measurement chamber and the differentially pumped chamber with a valve, adequate operation conditions can be created. Secondly, the differentially pumped section can be isolated from the other chambers during venting to prevent contamination of the QMS.

To be able to achieve an ultra high vacuum in the LiMeS-TDS device, heaters will be attached to the differentially

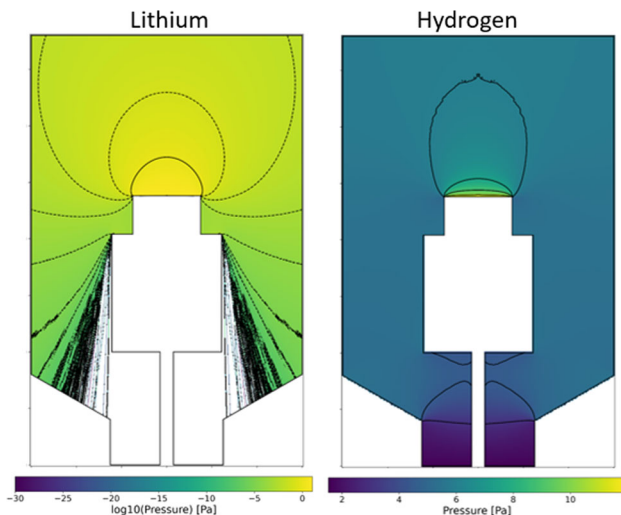


Fig. 5 Pressure simulated via the DSMC method of Lithium (left) and Hydrogen (right) in a conceptual geometry of the evaporation chamber. Note the logarithmic scale of the lithium pressure while the hydrogen pressure is given by a linear scale. The main difference between the two simulations, next to the gas type, is the absorbing boundary condition of the walls for the lithium while the hydrogen uses a reflective boundary condition. The evaporated amount of gas is equal to the particle flux of lithium evaporating into vacuum via the Langmuir–Knudsen equation at 650 °C

pumped chamber and the measurement chamber to perform a bake and desorb impurities from the vessel walls. Currently, the heating system with the calibration gas lines is under development to finalize the conceptual system design. Parallel to this, concepts are being developed to integrate the LiMeS-TDS device with an argon atmosphere glovebox. This will allow for placing, handling, and removing samples in LiMeS-TDS under a protected atmosphere, preventing lithium impurities from forming due to air exposure, as well as enable transport between different devices with a protected atmosphere via a sealed container.

Conclusion

In this paper, the design goals and concept of each of the four devices of LiMeS-Lab have been presented. With the devices as discussed, LiMeS-Lab will provide a testbed for research topics such as metal vapor and plasma interaction and liquid metal hydrogen/deuterium retention. Next to this, it provides the means and infrastructure to demonstrate the feasibility and capability of different PFC concepts being researched and developed. Therefore, LiMeS-Lab will be a key facility to take the next steps towards a liquid metal divertor.

Author Contributions Conceptualization, methodology and investigation of: LiMeS-AM: JAWD, MGDG and TWM; LiMeS-Wetting: RSA, MJP, MR, VFBT, and EGPV; LiMeS-PSI: RSA, SAW, SB, IGJC, HJNE, HJM, TWM, CAO, MJP, PR, TPR, JS, VFBT, RHMT, JWMV, and EGPV; LiMeS-TDS: SAW, MJP, VFBT, and JWMV. Supervision provided by: MGDG, TWM, and NJLC. Writing done by TWM, and VFBT. Review performed by all authors. Visualization done by VFBT. Project administration performed by TWM and MJP. Funding acquisition secured by TWM, HJNE, IGJC, HJM, PR, NJLC, JAWD and MGDG.

Data Availability The datasets generated during and/or analysed during the current study are available in the Zenodo repository: <https://doi.org/10.5281/zenodo.7680828>

Declarations

Conflict of interest DIFFER is part of the institutes organisation of NWO. This work is part of the research programme ‘LiMeS-lab: An integrated laboratory for the development of Liquid-Metal Shield technologies for fusion reactors’ with project number 175.2019.035, which is partly financed by NWO. This work has been carried out within the framework of the EUROfusion Consortium, funded by the European Union via the Euratom Research and Training Programme (Grant Agreement No 101052200 - EUROfusion). Views and opinions expressed are however those of the author(s) only and do not necessarily reflect those of the European Union or the European Commission. Neither the European Union nor the European Commission can be held responsible for them.

Open Access This article is licensed under a Creative Commons Attribution 4.0 International License, which permits use, sharing, adaptation, distribution and reproduction in any medium or format, as long as you give appropriate credit to the original author(s) and the source, provide a link to the Creative Commons licence, and indicate if changes were made. The images or other third party material in this article are included in the article’s Creative Commons licence, unless indicated otherwise in a credit line to the material. If material is not included in the article’s Creative Commons licence and your intended use is not permitted by statutory regulation or exceeds the permitted use, you will need to obtain permission directly from the copyright holder. To view a copy of this licence, visit <http://creativecommons.org/licenses/by/4.0/>.

References

1. G. Federici, W. Biel, M.R. Gilbert, R. Kemp, N. Taylor, R. Wenninger, Nucl. Fusion **57**(9), 092002 (2017). <https://doi.org/10.1088/1741-4326/57/9/092002>
2. H. Yamada et al., J. Fusion Energy. **35**(1), 4–26 (2016). <https://doi.org/10.1007/s10894-015-0018-1>
3. K. Kim et al., Nucl. Fusion **55**(5), 053027 (2015). <https://doi.org/10.1088/0029-5515/55/5/053027>
4. P. Rindt, J.L. van den Eijnden, T.W. Morgan, and N. J. Lopes Cardozo. Fusion Eng. Des. **173**(December), 112812 (2021). <https://doi.org/10.1016/j.fusengdes.2021.112812>
5. F.L. Tabarés, Plasma Phys. Control. Fusion **58**(1), 014014 (2016). <https://doi.org/10.1088/0741-3335/58/1/014014>
6. R.E. Nygren, F.L. Tabarés, Nucl. Mater. Energy **9**(December), 6–21 (2016). <https://doi.org/10.1016/j.nme.2016.08.008>
7. C.E. Kessel et al., Fusion Sci. Technol. **75**(8), 886–917 (2019). <https://doi.org/10.1080/15361055.2019.1610685>

8. D.G. Whyte, T.E. Evans, C.P.C. Wong, W.P. West, R. Bastasz, J.P. Allain, J.N. Brooks, *Fusion Eng. Des.* **72**(1–3), 133–147 (2004). <https://doi.org/10.1016/j.fusengdes.2004.07.014>
9. D.N. Ruzic, W. Xu, D. Andruczyk, M.A. Jaworski, *Nucl. Fusion* **51**(10), 102002 (2011). <https://doi.org/10.1088/0029-5515/51/10/102002>
10. T.W. Morgan, P. Rindt, G.G. Van Eden, V. Kvon, M.A. Jaworski, N.J. Lopes Cardozo, *Plasma Phys. Control. Fusion*, **60**(1), 014025 (2018). <https://doi.org/10.1088/1361-6587/aa86cd>
11. R.J. Goldston, R. Myers, J. Schwartz, *Phys. Scr.* **2016**(T167), 014017 (2016). <https://doi.org/10.1088/0031-8949/T167/1/014017>
12. Q. Yang et al. *Fusion Eng. Des.*, **124**(November), 179–182 (2017). ISSN 0920-3796. <https://doi.org/10.1016/j.fusengdes.2017.04.063>
13. R. Majeski et al., *Fusion Eng. Des.* **72**(1), 121–132 (2004). <https://doi.org/10.1016/j.fusengdes.2004.07.002>
14. S.V. Mirnov, V.A. Evtikhin, *Fusion Eng. Des.* **81**(1), 113–119 (2006). <https://doi.org/10.1016/j.fusengdes.2005.10.003>
15. M.A. Jaworski et al. *Nucl. Fusion*, (8), 083032 (2013). <https://doi.org/10.1088/0029-5515/53/8/083032>
16. A.V. Vertkov, I.E. Lyublinski, *Phys. At. Nucl.* **81**, 1000–1007 (2018). <https://doi.org/10.1134/S1063778818070141>
17. A. Kreter, C. Brandt, A. Huber, S. Kraus, S. Möller, M. Reinhart, B. Schweer, G. Sergienko, B. Unterberg, *Fusion Sci. Technol.*, **68**(1), 8–14 (2015). <https://doi.org/10.13182/FST14-906>
18. J.H. You et al., *Nucl. Mater. Energy* **16**(August), 1–11 (2018). <https://doi.org/10.1016/j.nme.2018.05.012>
19. T.W. Morgan, Y. Li, M. Balden, S. Brezinsek, G. De Temmerman, *Nucl. Fusion* **61**(11), 116045 (2021). <https://doi.org/10.1088/1741-4326/ac25c2>
20. P. Rindt et al. *Nucl. Fusion*, **59**(5) (2019). <https://doi.org/10.1088/1741-4326/ab0a76>
21. A. von Müller, G. Schlick, R. Neu, C. Anstatt, T. Klimkait, J. Lee, B. Pascher, M. Schmitt, C. Seidel, *Nucl. Mater. Energy* **19**(May), 184–188 (2019). <https://doi.org/10.1016/j.nme.2019.02.034>
22. E.A.I. Ellis, M.A. Sprayberry, C. Ledford, J.P. Hankwitz, M.M. Kirka, C.D. Rock, T.J. Horn, Y. Katoh, R.R. Dehoff, J. Nucl. Mater. **555**(November), 153041 (2021). <https://doi.org/10.1016/j.jnucmat.2021.153041>
23. J. Braun, L. Kaserer, J. Stajkovic, K.H. Leitz, B. Tabernig, P. Singer, P. Leibenguth, C. Gspan, H. Kestler, G. Leichtfried, *Int. J. Refract. Met. Hard Mater.* **84**(June), 104999 (2019). <https://doi.org/10.1016/j.ijrmhm.2019.104999>
24. J.G.A. Scholte, M. Iafrazi, S.S.H. Lam, B. Tyburska-Pueschel, M. Riepen, F. Brochard, M.M.P. Vissers, T.W. Morgan, *Nucl. Mater. Energy* **34**(March), 101315 (2023). <https://doi.org/10.1016/j.nme.2022.101315>
25. B. Vrancken, Rishi K. Ganeriwala, Aiden A. Martin, Manyalibo J. Matthews. *Addit. Manuf.*, **46**(October), 102158 (2021). <https://doi.org/10.1016/j.addma.2021.102158>
26. N. Eustathopoulos, *Metals* **5**(1), 350–370 (2015). <https://doi.org/10.3390/met5010350>
27. A. Warren, A. Nylund, I. Olefjord, *Int. J. Refract. Met. Hard Mater.* **14**(5–6), 345–353 (1996). [https://doi.org/10.1016/s0263-4368\(96\)00027-3](https://doi.org/10.1016/s0263-4368(96)00027-3)
28. H. Maecker, *Z. Naturforsch. A* **11**(6), 457–459 (1956). <https://doi.org/10.1515/zna-1956-0606>
29. G.M.W. Kroesen, D.C. Schram, M.J.F. van de Sande, *Plasma Chem and Plasma Process* **10**(1), 49–69 (1990). <https://doi.org/10.1007/BF01460447>
30. W.A.J. Vijvers, D.C. Schram, A.E. Shumack, N.J. Lopes Cardozo, J. Rapp, G.J. Van Rooij, *Plasma Sources Sci. Technol.*, **19**(6), 065016 (2010). <https://doi.org/10.1088/0963-0252/19/6/065016>
31. R.M. Wang, S.C., van der Horst, M. van Kampen, T.W. Morgan. *Plasma Sources Sci. Technol.*, **31**(8), 85011 (2022). <https://doi.org/10.1088/1361-6595/ac71c3>
32. J.F.M. Velthuis, A. Storm, M. van Kampen, R. van der Horst, H.B. Profijt, *J. Vac. Sci. Technol.* **37**(6), 61302 (2019). <https://doi.org/10.1116/1.5120339>
33. M.J. Baldwin, T. Lynch, L. Chousal, R.P. Seraydarian, R.P. Doerner, S.C. Luckhardt, *Fusion Eng. Des.* **70**(2), 107–113 (2004). [https://doi.org/10.1016/S0920-3796\(03\)00415-0](https://doi.org/10.1016/S0920-3796(03)00415-0)
34. G.G. Van Eden, T.W. Morgan, D.U.B. Aussems, M.A. van den Berg, K. Bystrov, M.C.M. van de Sanden, *Phys. Rev. Lett.* **116**, 135002 (2016). <https://doi.org/10.1103/PhysRevLett.116.135002>
35. H.J.N. van Eck et al., *Fusion Eng. Des.* **142**(May), 26–32 (2019). <https://doi.org/10.1016/j.fusengdes.2019.04.020>
36. G.G. Van Eden, T.W. Morgan, H.J. Van Der Meiden, J. Matejicek, T. Chraska, M. Wirtz, G. De Temmerman, *Nucl. Fusion* **54**(12), 123010 (2014). <https://doi.org/10.1088/0029-5515/54/12/123010>
37. E. Oyarzabal, A.B. Martín-Rojo, F.L. Tabarés, *Fusion Eng. Des.* **117**, 217–221 (2017). <https://doi.org/10.1016/j.fusengdes.2016.08.009>
38. M. Christenson, D. Panici, C. Moynihan, J. Wendeborn, J. Anderson, D.N. Ruzic, *Nucl. Fusion* **59**(2), 026011 (2019). <https://doi.org/10.1088/1741-4326/aaf587>
39. J. Knaster, T. Kanemura, K. Kondo, *Heliyon* **2**(12), e00199 (2016). <https://doi.org/10.1016/j.heliyon.2016.e00199>
40. A. De Castro, A. Sepetys, M. González, F.L. Tabarés, *Nucl. Fusion* **58**(4), 046003 (2018). <https://doi.org/10.1088/1741-4326/aaa8d0>
41. D.W. Jeppson, J.L. Ballif, W.W. Yuan, B.E. Chou. *Lithium Literature Review: Lithium’s Properties and Interactions.* 4 (1978). <https://doi.org/10.2172/6885395>
42. S.J. Plimpton, S.G. Moore, A. Borner, A.K. Stagg, T.P. Koehler, J.R. Torczynski, M.A. Gallis, *Phys. Fluids* **31**(8), 86101 (2019). <https://doi.org/10.1063/1.5108534>
43. J.A. Schwartz, E.D. Emdee, R.J. Goldston, M.A. Jaworski, *Nucl. Mater. Energy* **18**(January), 350–355 (2019). <https://doi.org/10.1016/j.nme.2019.01.024>

Publisher’s Note Springer Nature remains neutral with regard to jurisdictional claims in published maps and institutional affiliations.